SPARSE-LAYER INVERSION AS A TOOL TO DELINEATE THIN SANDSTONES, LOWER MAGDALENA VALLEY REGION, COLOMBIA: A CASE STUDY

A Thesis Presented to

the Faculty of the Department of Earth & Atmospheric Sciences

University of Houston

In Partial Fulfillment

of the Requirements for the Degree

Master of Science

By

Jorge Andrés Donoso

December 2016

SPARSE-LAYER INVERSION AS A TOOL TO DELINEATE THIN SANDSTONES, LOWER MAGDALENA VALLEY REGION, COLOMBIA: A CASE STUDY

Jorge Andrés Donoso

APPROVED:

Dr. John P. Castagna, Chairman
Dept. of Earth and Atmospheric Sciences

Dr. Evgeny Chesnokov
Dept. of Earth and Atmospheric Sciences

Dr. Roderick Perez
Pacific Exploration & Production

Dean, College of Natural Sciences and Mathematics

Acknowledgments

I wish to express my appreciation to Dr. John Castagna for his guidance and allowing me to be his student, and to my thesis advisors Dr. Evgeny Chesnokov, and Dr. Roderick Perez for their recommendations and advice throughout the thesis process. My gratitude also goes to Lumina Geophysical and Mr. Carlos Moreno for allowing me the use of their proprietary software technology to perform my thesis research. I want to thank all the Lumina Geophysical team, especially Mr. Gabriel Gil for his helpful comments on my thesis results. Thanks to Pacific Exploration & Production for its permission to use and present their data. I also wish to thank all my family and friends for their unconditional support during my time at the University of Houston. Special thanks to Mr. Luis Melo and Dr. Lucetti for their logistic assistance to bring this thesis to a successful conclusion.

SPARSE-LAYER INVERSION AS A TOOL TO DELINEATE THIN SANDSTONES, LOWER MAGDALENA VALLEY REGION, COLOMBIA: A CASE STUDY

An Abstract of a Thesis

Presented to

the Faculty of the Department of Earth & Atmospheric Sciences

University of Houston

In Partial Fulfillment

of the Requirements for the Degree

Master of Science

By

Jorge Andrés Donoso

December 2016

Abstract

Recent oil and gas exploration in the Lower Magdalena Valley, Northern Colombia, has shown the presence of gas in the Lower Porquero shale formation. The existence of thin hydrocarbon-filled reservoir sandstones below seismic resolution can explain the seismic response. To test this hypothesis, seismic response is modeled near existing wells and compared with high-resolution data generated by a sparse-layer reflectivity inversion, constrained by high-resolution spectral decomposition, applied to conditioned pre-stack seismic data from the La Creciente block at northern Magdalena region of Colombia. Seismic-data-conditioning algorithms, such as structural and radon filtering, were tested, calibrated, and applied to the pre-stack seismic gathers as a preliminary step before implementing the sparse-layer reflectivity inversion. Removal of incoherent noise and processing artifacts is crucial prior to the application of the sparse-layer seismic reflection inversion to guarantee high-quality results whilst preserving AVO behavior and honoring existing faults. The increased frequency bandwidth and improved resolution allowed the detection of events previously not seen on the seismic data that may delineate unexplored potential gas reservoirs.

Contents

List of Figures

List of Tables

Chapter 1

Introduction

1.1 Motivation and Objective

During the hydrocarbon exploration in the Cienága de Oro formation, presence of gas was detected in thin sandstone layers embedded in the Lower Porquero formation, which is comprised mostly of shale and sits on top of the Cienága de Oro formation. These gas-filled thin-sandstone layers are of great significance for hydrocarbon exploration. The main area of interest, and where the gas presence was strongly identified, corresponds to Well-B at 9800 ft depth and Well-C at 10825 ft depth as can be seen in Figure 1.1. The measured thickness of the sandstone packets of interest is between 30 ft and 60 ft. The theoretical limit of seismic resolution of thin layers is $\lambda/8$ (here λ represents wavelength), a practical limit is $\lambda/4$, below which top and base of a layer cannot be resolved (Widess, 1985). Calculating from measured P-wave velocity of approximately 9500 ft/s and the mean seismic frequency 20 Hz at the target depth

and location, the expected $\lambda/4$ resolution limit is roughly 120 ft, not enough to be able to detect the layers of interest.

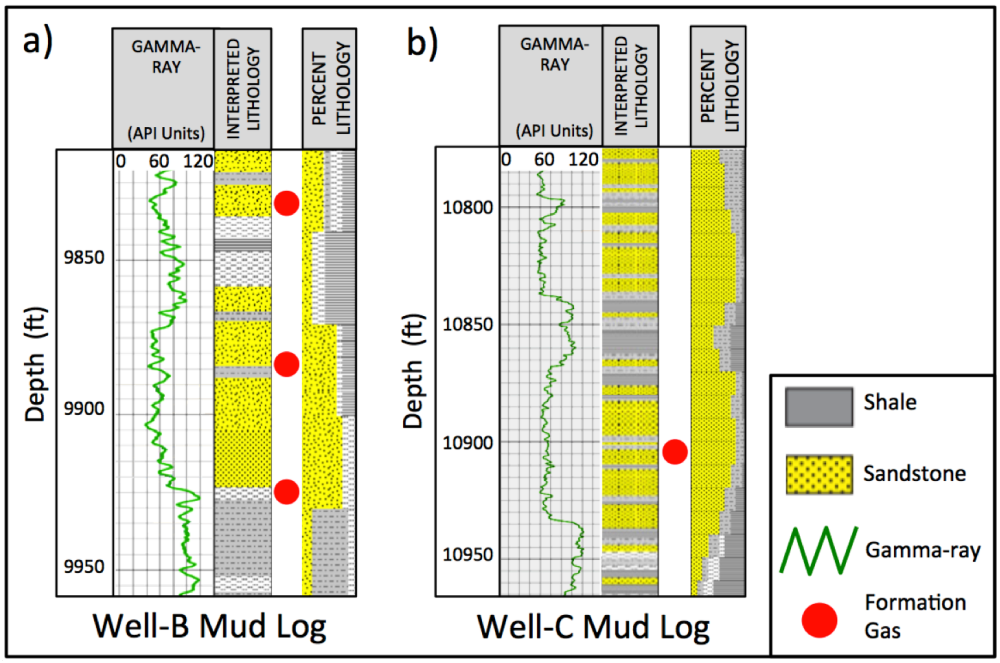

Figure 1.1: Mud Logs at Area of Interest. (a) Well-B mud log. (b) Well-C mud log. Red dots indicate presence of gas in layers of interest. Courtesy of Pacific Exploration & Production.

My hypothesis is that the seismic response in these areas is explained by the existence of thin layers below seismic resolution. This will be tested using well logs and with seismic modeling; the target and focus of this thesis work will then be to increase the seismic data resolution of the target area to better detect or visualize these thin sandstones. The tool selected for this is a pre-stack sparse-layer reflectivity inversion method developed by Zhang and Castagna (2011). By applying the sparse-layer reflectivity inversion to the seismic data obtained after data-conditioning, previously unseen layers could be detected, making possible the delineation of the sandstone layers in the area of interest.

1.2 Geological Overview

The geological overview and the stratigraphic column (Figure 1.2) are modified from the Colombian Sedimentary Basins reference book published on 2007 by the Colombian National Agency for Hydrocarbons (hereafter ANH).

The Lower Magdalena Basin is located in the northwest of Colombia where oblique subduction along the Romeral fault system has produced transpressional and transtensional deformation from the late Cretaceous to present day. The Lower Magdalena Basin is limited to the northeast by the Bucaramanga - Santa Marta fault system; to the south by the Central Cordillera and to the west by the Romeral fault system. This basin is subdivided by three structural elements that have controlled sedimentation since Eocene to late Miocene. These structural elements are: The Plato sub-basin to the north, the Cicuco Arch in the central part, and the San Jorge sub-basin to the south. The Lower Porquero Formation, an Early Miocene shale, has been recognized as the main source of hydrocarbons in the basin. This is a thick shale, rich in organic matter and type II kerogen. The Cienága de Oro Formation has an upper interval with fair-to-rich content of type III organic matter, within the oil window in the deepest areas of the basin. This interval could be considered as deposited during a maximum flooding event. The available source rock data suggests a pod of active source rock, probably of Cretaceous age, coinciding with the areas of greater sediment depth. These pods of active source rock in the generation/expulsion phase are present in an extensive area in the so-called Plato sub-basin; between the

wells Guamito-1 to the northeast and Pijino-1 to the south. API gravity for oil generated within the basin varies between 30° to 52°. The sulfur content is very low; while the paraffin concentration is relatively high. Various geochemical parameters indicate that the majority of oil originated in a relatively dioxic proximal siliciclastic environment. Four different migration pathways have been proposed: 1) The Cicuco-Boquete area. 2) Momposina area. 3) Guepaje area and 4) Apure-region. Migration most likely happens along a network of fracture and fault planes. The Cienága de Oro Formation, composed of Oligocene sandstones and limestones, is the main reservoir in the basin, with a 300 ft gross thickness and average porosity of 15%. Shales of the upper Porquero and Cienága de Oro formations deposited during a period of rapid subsidence, have excellent physical characteristics as a sealing unit. The deep-water shales are the regional top seal for the under-laying reservoir rocks. The younger Tubará Formation (Middle Miocene to Lower Pliocene) is also a sealing unit. Diverse types of structural trap highlight the basin potential, among others: structural traps associated with high-side closures in contractional faults, anticline closures in the footwall of normal faults, structures related to flower geometries generated by transpression, roll-overs in the hanging-wall of listric normal faults, all of them are important structural exploration targets in the basin. Stratigraphic traps are also of great economic impact, since production from carbonates has long been established and submarine fan turbidites are also prospective. Presence of oil fields and abundant oil seeps, together with a great variety of structural traps and recent generation from pods of active source rock in deep synclinal structures indicate very good potential for discovery of new reserves. In this basin 117 wildcat wells have

been drilled; and approximately 20,300 lineal kilometers of seismic data have been acquired. With 17 oil field discoveries and tested oil reserves of 71 MMbbl (until December 2005) it is a very promising area for further exploration.

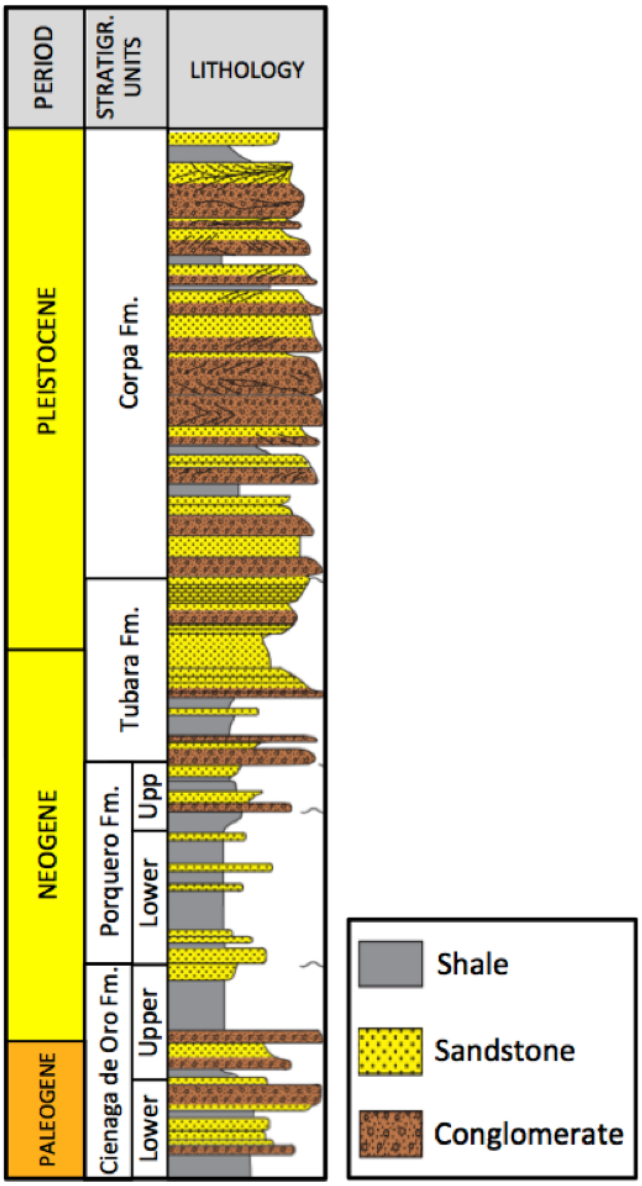

Figure 1.2: Stratigraphic Column. Modified from ANH, 2007.

1.3 Available Data

The original available data includes pre-stack offset gathers, an interval velocity volume and well logs. The pre-stack seismic data covers a total of 203.81 km^2 in the study area located near the Sincelejo city in the Sucre department, Colombia. Figure 1.3 shows the relative location of the area of study.

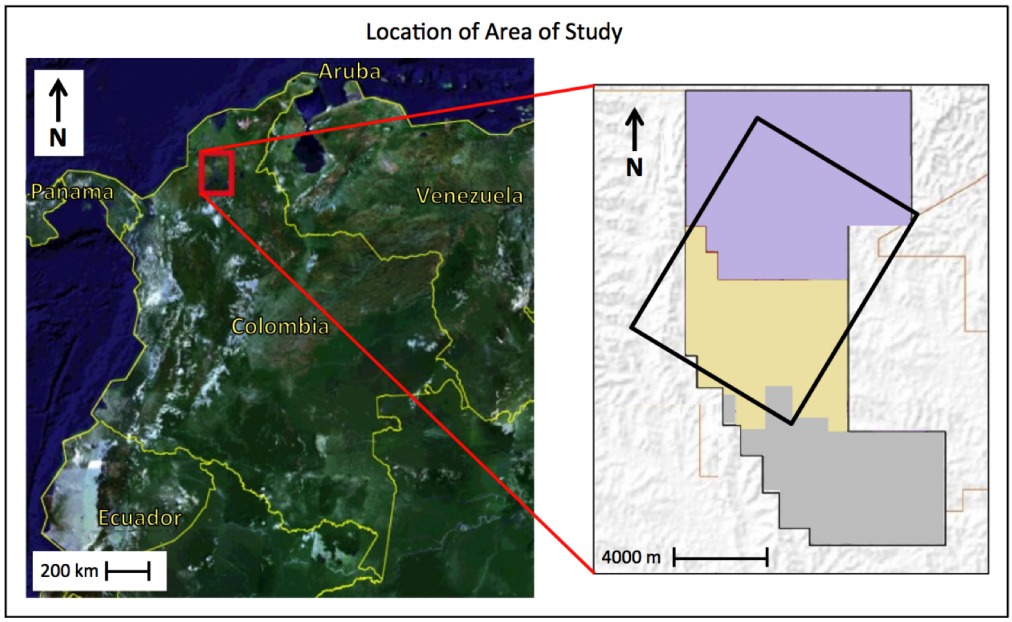

Figure 1.3: Location of Area of Study. La Creciente Block, Lower Magdalena Valley, Colombia. Available seismic data in black rectangle. Modified from www.igac.gov.co and courtesy of Pacific Exploration & Production.

The pre-stack offset gathers exhibit very high random noise, in particular at high frequencies; as if noise had been blown-up by a failed attempt at increasing the high-frequency content of the data (see Figure 1.4). Although seismic events are visible in the area of interest, the poor data quality motivated the application of a dedicated data-conditioning sequence to improve the signal-to-noise ratio of the data. A more detailed analysis is presented in Chapter 2.

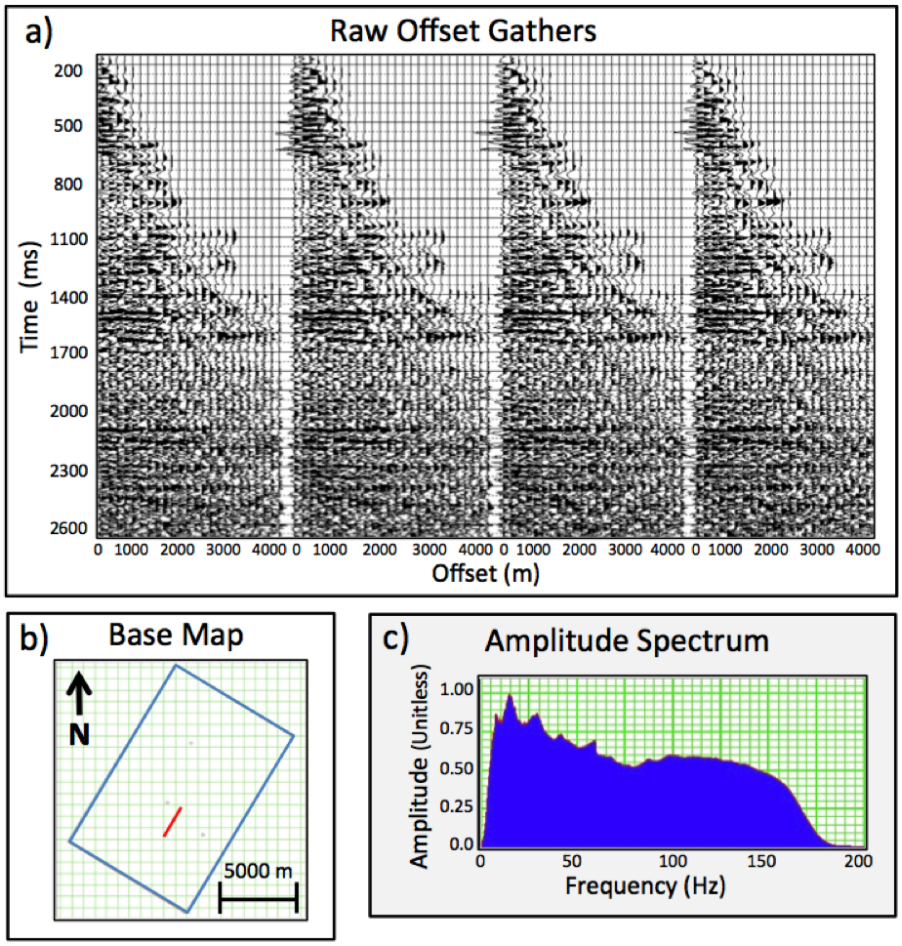

Figure 1.4: Raw Data. (a) Raw pre-stack offset gathers. (b) Location on base map. (c) Amplitude spectrum. All amplitudes are relative and thus unitless.

On the provided velocity volume an artifact was detected at shallow locations; a value of 5000 m/s that did not make any sense at this depth, it was necessary to correct these unwanted values and replace them with appropriate velocities at shallow depths. It is fortunate that this artifact did not affect the target area; regardless it was necessary to make this correction in order to have an accurate incident angle modeling. An additional benefit of reviewing the velocity model is the optimization of offset to angle conversion, since AVO equations are a function of incidence angles.

Approximately 10 wells are part of the original available data; only 3 of them, referred in this work as Well-A, Well-B, and Well-C; had existing P-wave logs in the target formation and were used (see Table 1.1). Of these Well-B did not have an S-wave log and had to be calculated using the mudrock equation (Castagna, 1985) and Well-C lacked a density log in which case it was calculated using Gardner's density equation (Gardner, 1974).

Well Name	**Gamma Log**	**Density Log**	**P-Wave Log**	**S-Wave Log**
Well-A	x	x	x	x
Well-B	x	x	x	
Well-C		x	x	x

Table 1.1: Well Logs Selected.

1.4 Dissertation Overview

Chapter 2 begins by observing that the pre-stack data has very low signal-to-noise ratio, high-frequency noise content and low fold (Figure 2.1).

Before the sparse-layer reflectivity inversion is applied, a pre-stack data-conditioned process was implemented on the seismic data with the main objective of improving signal-to-noise ratio. Chapter 2 summarizes this process, which consists of roughly 7 steps of filter applications on offset pre-stack gathers and finally offset-to-angle conversion. During the sequence, every filter applied was submitted to a careful quality

control (hereafter QC) of its parameters in order to reduce the chances of removing useful signal whilst eliminating unwanted noise and artifacts. After the application of each filter, far offsets and near offsets were stacked to compare the improvement in structural continuity after each step, and later subtracted to visualize the residual both in the gathers and in the stack and to confirm that no coherent information, flat events, or obvious geological information was removed; this was done for each of the filters but only the main results will be shown here. Among other QC steps done were AVO gradient analysis on the layers of interest before and after each of the filter applications to guarantee that AVO behavior was preserved; most importantly for the filters that enhance structure by flattening events on the gathers or smoothing along structure. Well-ties were done at the beginning using the existing P-wave logs to define a depth-time curve to adjust and calibrate the depth in feet from the logs to the time depth of the seismic and thus be able to indicate properly the location and depth of particular events of interest.

Chapter 3 builds on the data-conditioning sequence results as input for the sparse-layer reflectivity inversion to generate a data volume rich in high-frequency with improved resolution of events. On the input data, the mean frequency was 30 Hz and the desired frequency increase was to double the bandwidth. Parameter selection for horizontal continuity and vertical resolution increase was done observing that if the horizontal continuity was forced it would eliminate existing faults and vertically it would generate high-resolution artifacts, both of which would have yielded undesired results. Wedge models were created for odd reflectivity layer couples using the extracted wavelet from the data, first from the conditioned data and then using a 60 Hz

Ricker wavelet. This was done to test the assumption that the target frequency is able to resolve the events of interest; and indeed a detailed analysis of synthetic traces near the existing wells at the depth of interest shows seismic events that were previously not seen and are consistent with the mud logs where the presence of gas was detected. QC included well-ties that were observed after the sparse-layer inversion to analyze consistency with the previous well-tie correlation to the conditioned data, as well as AVO behavior monitored at several areas of the resulting volume; but in particular at the locations with detected presence of gas at Well-B and Well-C. Other QC processes were to shape the amplitude spectrum of the inverted data to match that of the input data and to convolve the inverted data with a wavelet extracted from the conditioned data results, both showing high similarity and validating the results form the sparse-layer inversion method at La Creciente block.

Chapter 4 summarizes the conclusions of the previous chapters regarding the necessity of a pre-stack data-conditioning sequence application, the validity of the sparse-layer reflectivity inversion method used on data from the Lower Magdalena valley and its correlation with the existing well log information.

Chapter 2

Data Conditioning

2.1 Introduction

Target-oriented data conditioning is a basic and first step in any reservoir characterization workflow and if done correctly, the results of seismic inversion are greatly improved (Estrada, 2016). Seismic inversion methods used for reservoir characterization are ultimately dependent on the quality of the input seismic data (Schmidt et al. 2013). The ideal seismic data should be rich in high-frequency and low-frequency content, with flat events and without noise. Removing noise on the pre-stack gathers results in a higher resolution and lateral continuity of the inverted result (Zhang et al. 2015).

Is important to avoid removing valid signal that contains geological and geophysical information during the process of reducing coherent noise being the main

objective to increase signal-to-noise ratio. Although it is assumed that most coherent noise is properly dealt with during the data-processing stage, the use of pre-stack procedures for noise attenuation, as for example Radon transform filtering, have proven quite useful (Schmidt 2013). This provides better insight and confidence in the input seismic data and final results of the inversion methods that lead to an improved interpretation (Schmidt 2013). Because of this, gather conditioning is seen by many as a prerequisite to pre-stack seismic inversion (Singleton, 2009) as noise is stronger on pre-stack gathers than in post-stack data. Noise suppression is also needed to accurately flatten seismic events in the offset gathers whilst preserving AVO behavior in preparation for a seismic inversion (Chopra and Castagna, 2014).

In this thesis, synthetic gathers, time-slice maps, residual plots, and stacking are used to QC a conditioning sequence that is adequate for the eventual application of the sparse-layer reflectivity inversion technique. In each processing step, the output will be compared to the raw data and improvement in data quality assessed. The first step in the conditioning sequence will be to remove unwanted noise in the seismic gathers, thus enhancing signal-to-noise ratio mainly through bandpass filtering and the application of an angle mute. The next step will be to separate signal from reflection multiples and other coherent or random noise which may have remained after the data processing using the Radon transform, a structural filter is also used to further attenuate noise that is not coherent spatially and to flatten events on pre-stack gathers. Finally; an AVO filter will map the original AVO trend on the gathers and enhance it so that the input to the inversion process is consistent with the forward model used by the inversion. All the steps in the data conditioning

were submitted to QC mostly by subtracting the input and output gathers as well as subtracting the input and output stacks after each step and observing that the residual did not contain any information with geological behavior. Pre-stack seismic-data-conditioning should be a first and important step towards the goal of improving vertical resolution by using the sparse-layer inversion method proposed by Zhang and Castagna (2011), who developed the algorithm in order to resolve layers below conventional seismic resolution. The application of this will allow the resolution of events below tuning thickness in the Lower Porquero Formation. Figure 2.1 shows that the input angle gathers although filled with random noise still present consistent flat seismic events from the shallow depths and into the area of interest is the Lower Porquero formation, which is located at a time-depth between 2.2 and 2.5 seconds.

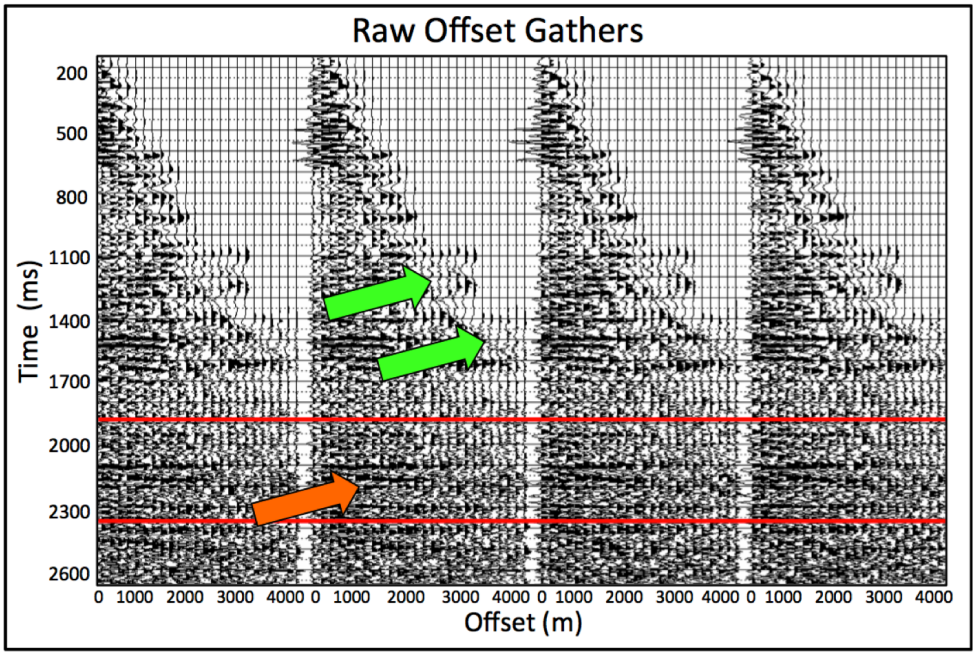

Figure 2.1: Raw Offset Gathers. The area of interest is indicated by the two red lines, notice the high content of noise post-critical angle (green arrows). The seismic reflection events are noticeable but clouded by low signal-to-noise ratio (orange arrow).

2.2 Workflow

Velocity volume. A simple but first step is to review the provided velocity volume and check its overall consistency. This is necessary to achieve an accurate incident angle calculation needed for inversion. An additional benefit of reviewing the velocity model is the optimization of offset to angle conversion, since AVO equations are a function of incidence angles (Schmidt et al. 2013).

High-cut filter. Looking at the amplitude spectrum of the raw seismic offset gathers on Figure 2.2 we can notice unexpected high-frequency values above 75 Hz, albeit these values are not natural to either raw or processed seismic data. This appears to be an processing artifact or a failed attempt at increasing the high-frequency content in the data processing stage for which there is no processing report available; it was necessary to remove these frequencies using a high-cut filter 50-80 Hz. To guarantee that by applying this filter no valuable seismic information was removed we subtracted the near and far offset stacks before and after the the high-cut filter, proving that only noise and no actual geological information was removed.

Angle Mute. To avoid the effects of serious stretch associated with large offsets, we usually mute the farthest offsets based on a user-define stretch criterion (Zhang et al. 2015). In order to apply an appropriate mute, that removes far offset noise whilst preserving as much useful information as possible, a synthetic gather was generated using a 20 Hz Ricker wavelet, which is the dominant frequency for the seismic data in the interval of interest, it indicated a critical angle at approximately 45 degrees, hence this angle mute was applied.

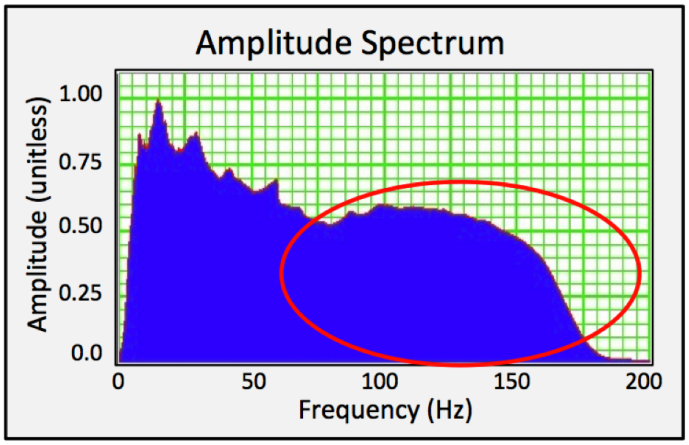

Figure 2.2: Raw Offset Gather Amplitude Spectrum. Notice the unusual high-frequency (red circle). All amplitudes are relative and thus unitless.

Multiple removal. In cases when data is severely contaminated by multiples, the Radon transform is a popular tool for regularization and preprocessing of seismic data prior to migration, AVO analysis and stratigraphic interpretation (Feng and Bancroft, 2006). The Radon transform filtering maps events into the tau-p space, where events with specific moveout can be enhanced or removed. Two parameters for the Radon transform filter need to be tested, since each seismic dataset is unique (Schmidt et al. 2013). The first is the time window of acceptable moveouts and second is the reference offset distance. The residual between original and Radon filtered gathers is inspected to be sure that no primary events are adversely affected by the filter (Figure 2.3). The residual was stacked to find that no coherent geological information was eliminated. Several values were tested but after analyzing the residual results the most effective choice of maximum moveout at the reference offset distance 2500 m was 50 ms.

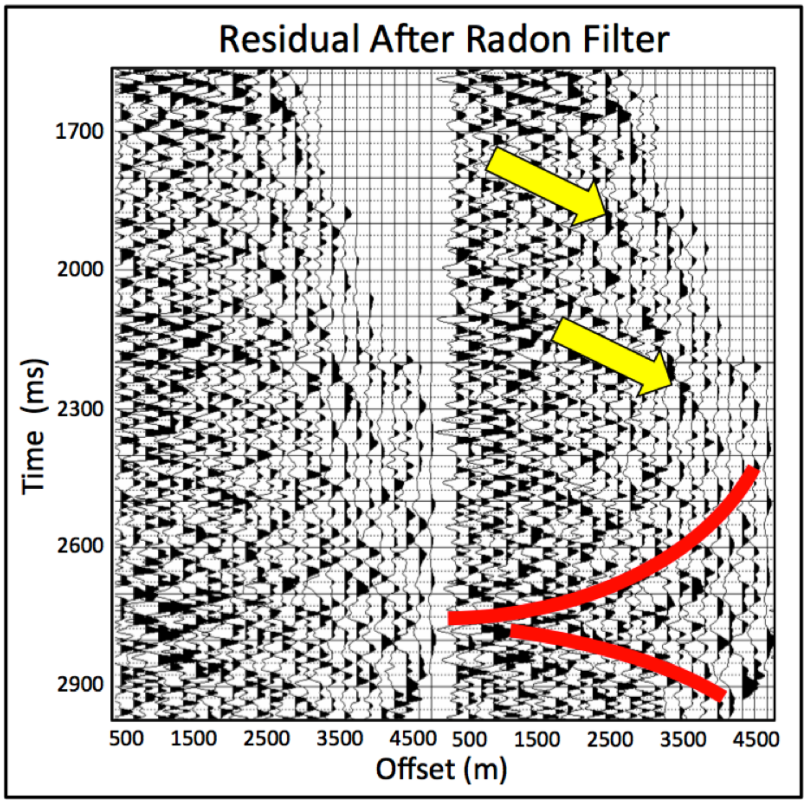

Figure 2.3: Residual Offset Gathers After Radon Filter. Notice no flat events were removed; Observe ground roll type noise (yellow arrows) and reflection multiples (red curves) were eliminated.

Event continuity. A structural filter was applied in order to improve the continuity of events. Structural filtering is based on the process of generating common offset stacks and measuring geometrical events properties such as dip and strike of events around individual traces on a small grid to follow geological events based on a semblance attribute (Chopra and Marfurt, 2007); slight corrections can then be made to flatten the events on pre-stack gathers. A small sampling window with median filtering is preferred to guarantee that no faults are being removed by oversmoothing; in this work a 5x5 traces sample window was used.

AVO gradient. One of the most important objectives of seismic-data conditioning is to preserve the AVO behavior on the seismic gathers. An AVO filter works by mapping the existing AVO response for the angle gathers and finding a best least-mean-squared fit to the Aki-Richards 2 term approximation, then producing a forward prediction using the obtained coefficients. This removes any remaining noise that is incompatible with the forward model in the inversion.

During the gather conditioning the AVO response for the target areas was monitored before and after each tested step. Figure 2.4 shows that the AVO behavior is not only maintained during the conditioning process but also enhanced in the target area.

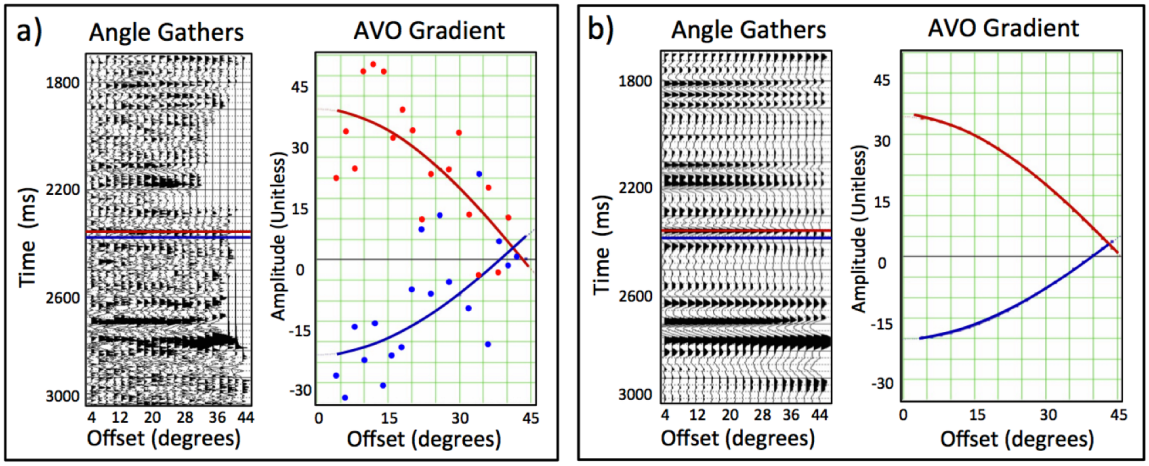

Figure 2.4: AVO Gradient Analysis of Seismic Angle Gathers. a) Raw data at Well-B location at 2350 ms. b) Conditioned data at Well-B location at 2350 ms. Notice that the AVO behavior is preserved and enhanced throughout all the conditioning process. Red curve is the least-mean-squared fit to the amplitude values sampled (red dots) in the top seismic event (red horizontal line). Blue curve is the least-mean-squared fit to the amplitude values sampled (blue dots) in bottom seismic event (blue horizontal line). All amplitudes are relative and thus unitless.

2.3 Results and Discussion

Each of the filters applied during the data conditioning process was controlled in order to not remove valuable seismic information. The result was a significant increase in signal-to-noise ratio and visual improvement of seismic events in the areas of interest as seen in Figure 2.5.

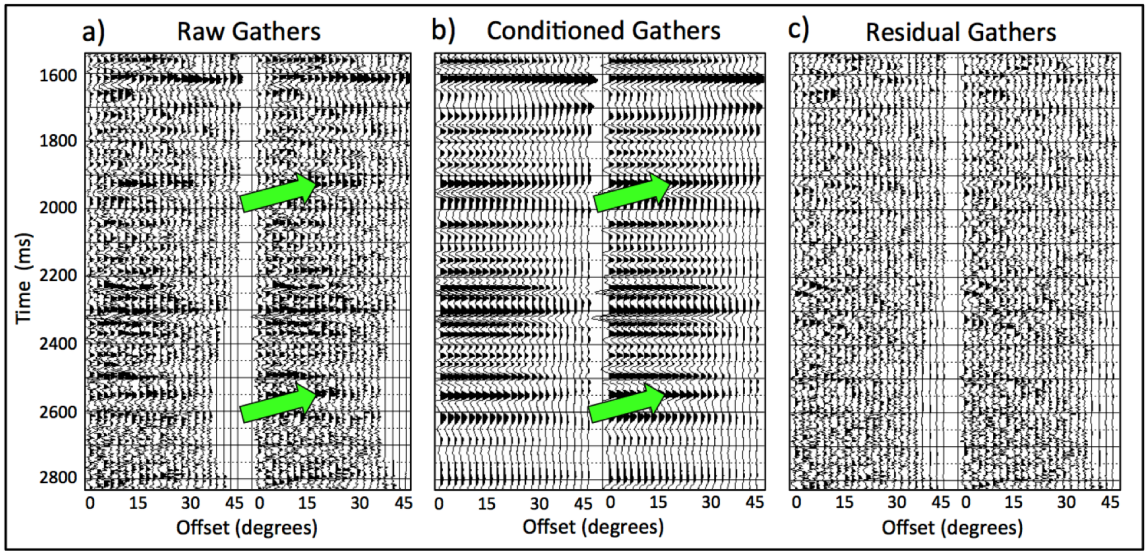

Figure 2.5: Condtioned Angle Gathers Results. (a) Raw seismic angle gathers. (b) Conditioned seismic angle gathers. (c) Residual gathers after conditioning. Notice increased continuity and visibility in angle gathers after conditioning (green arrows). No coherent flat events (primaries) are evident on the residual.

The gathers were stacked and subtracted to observe the effect of the conditioning sequence on the overall data. Figure 2.6 compares the stack before and after the conditioning process, improvement in the signal-to-noise ratio is evident as well as increased continuity in seismic events and removal of high-frequency noise; the original faults were preserved and random noise was removed, while preserving existing seismic events.

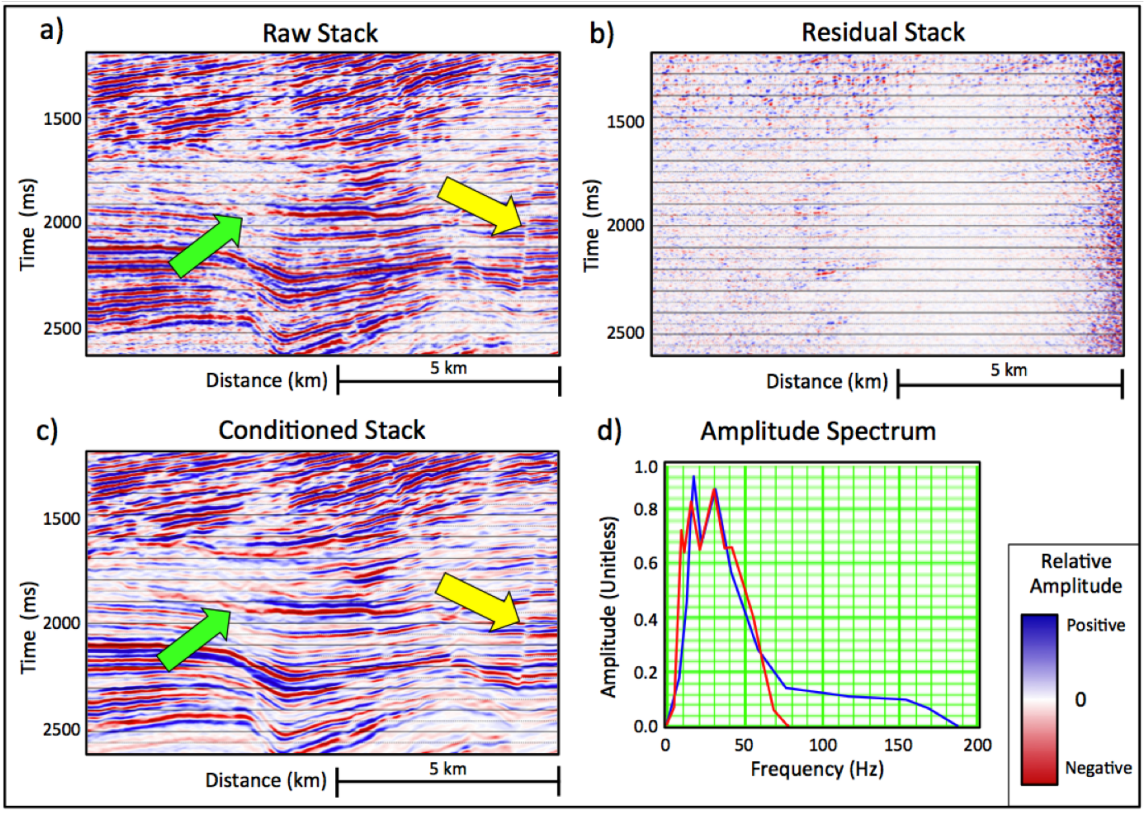

Figure 2.6: Conditioned Stack Results. (a) Raw stack. (b) Conditioned stack. (c) Residual stack after conditioning. (d) Amplitude spectra, the blue and red curves correspond to raw and conditioned data respectively. Notice an overall random noise reduction, increased continuity after conditioning (green arrows) and fault preservation (yellow arrows). All amplitudes are relative and thus unitless.

Figure 2.7 displays time slices at time 2200 ms before and after the conditioning process. The overall structure is preserved with a noticeable improvement in delineation of channels and faults. Well-ties were evaluated in the area of interest, showing a slight but positive improvement of the correlation of synthetic gathers with the stacks when comparing the raw seismic data and the conditioned seismic data.

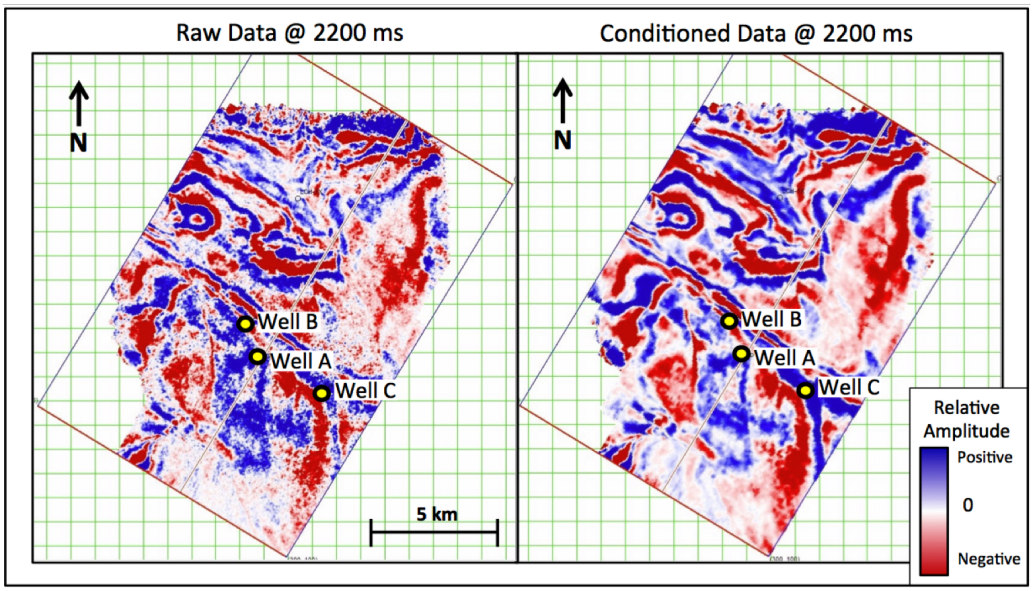

Figure 2.7: Conditioned Data Time Slice at 2200ms. (Left) Raw data . (Right) Conditioned data. All amplitudes are relative and thus unitless .

Figure 2.8 corresponds to Well-A well-tie, notice the correlation of the synthetic trace with seismic data was slightly improved in the area of interest. See Table 2.1 for well-tie correlation coefficients before and after the data-conditioning process.

Well Name	**Raw Coefficient**	**Conditioned Coefficient**
Well-A	0.816	0.864
Well-B	0.718	0.768
Well-C	0.621	0.683

Table 2.1: Well-tie Correlation Coefficients.

To demonstrate the improvement and advantage that comes from the proposed data-conditioning workflow, the pre-stack sparse-layer seismic inversion (Zhang and Castagna, 2011) was applied on the pre-stack gathers before and after the conditioning sequence, to make for a fair comparison identical parameters were used on both cases. The main discussion about the fundamentals of this particular seismic-inversion method and its advantages are explored in more detail in the next chapter. Notice in Figure 2.9 that, when applied to the raw data, the noise content increased significantly, even to the point of overshadowing layers in the target area. Data conditioning is evidently pivotal before attempting the seismic inversion process.

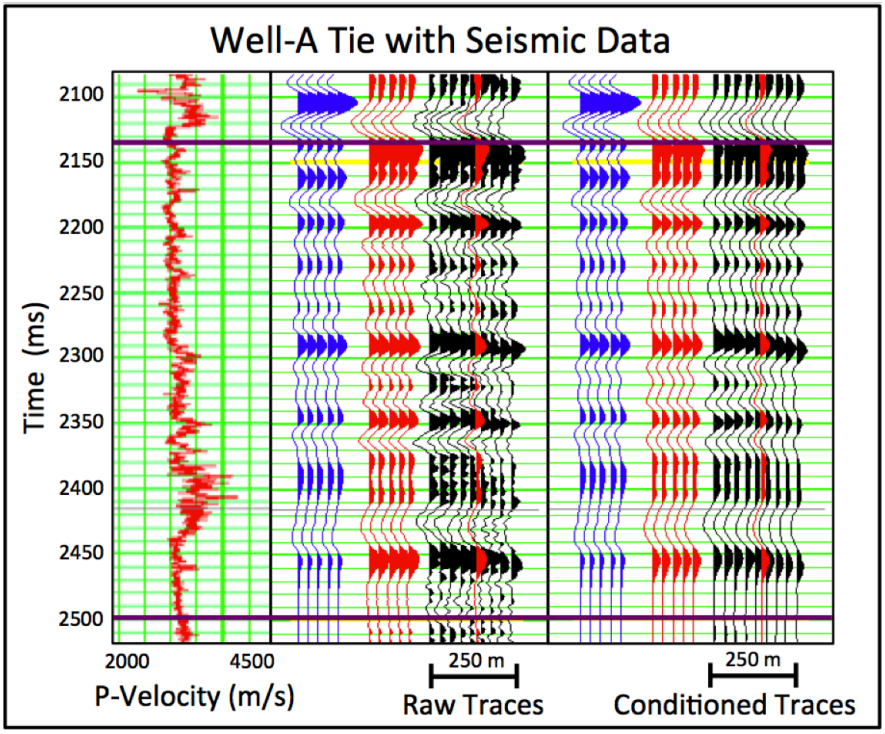

Figure 2.8: Well-A Well-tie Correlation. (Left) P-wave log . (Middle) Well-tie of Well-A with raw data. (Right) well-tie with conditioned data. Comparing synthetic trace (blue) with trace extracted from seismic data (red), seismic data used for correlation (black). Area of interest between the purple lines.

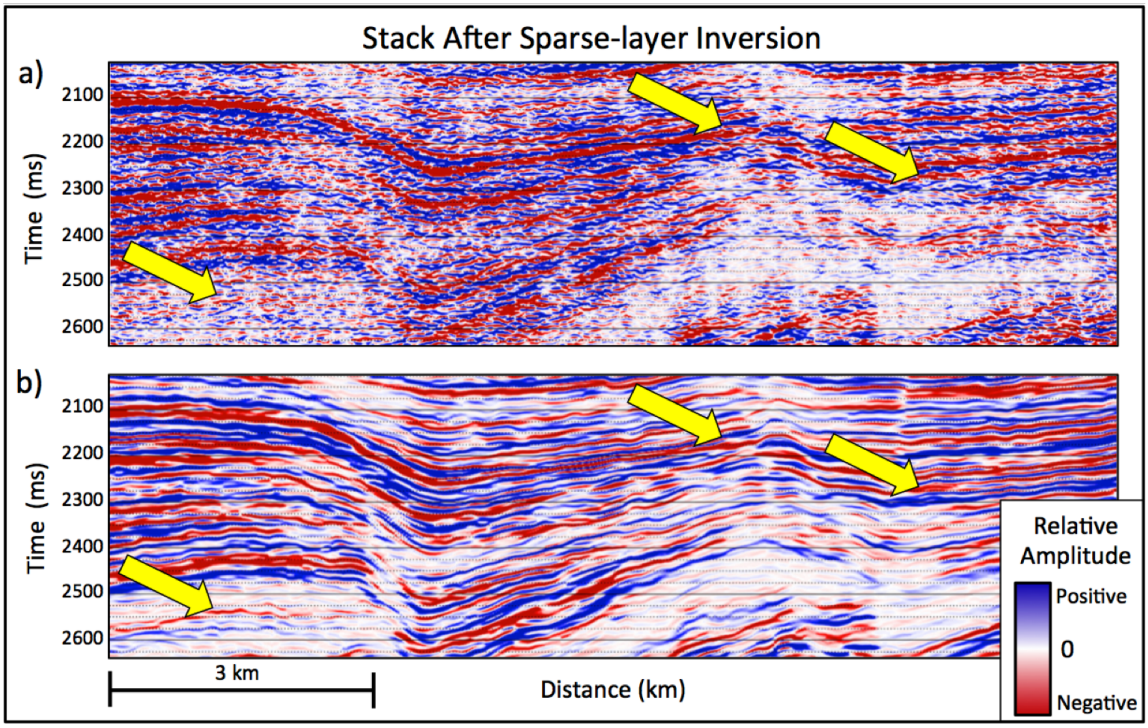

Figure 2.9: Stack After Sparse-layer Inversion. (a) Applied on raw seismic data. (b) Applied on conditioned seismic data. Noise was blown-up when raw data was used as input for sparse-layer inversion, hiding the events of target areas (yellow arrows). All amplitudes are relative and thus unitless.

Chapter 3

Sparse-layer Reflectivity Inversion

3.1 Introduction

Pre-stack seismic inversion techniques provide valuable information related to rock properties, lithology, and fluid content for reservoir characterization (Zhang and Marfurt, 2015), allowing the interpreter to visualize thin layers not readily seen on conventional seismic sections (Zhang and Castagna, 2011). Partyka et al. (1999) and Marfurt and Kirlin (2001) showed the possibility of using a discrete Fourier transform as a thickness-estimation tool; although these methods have limitations depending on the seismic bandwidth. Puryear and Castagna (2008) show that if reflection coefficients are determined simultaneously, the result is a sparse-reflectivity inversion method that can be parameterized to provide robust layer-thickness estimates. They exploit the fact that, in the frequency domain, the spacing between spectral peaks and notches is precisely the inverse of the layer thickness in the time domain (Partyka

et al., 1999; Marfurt and Kirlin, 2001), hence a spectral decomposition method that is able to provide accurate frequency spectra for seismic events assists in extending high frequencies without boosting noise beyond the original bandwidth of the data.

The presence of gas found in the thin layers below seismic vertical resolution in the Lower Porquero formation might indicate significant stratigraphic reservoirs or important flow units within reservoirs that have not yet been explored (ANH, 2007). When applying the sparse-layers reflectivity inversion on the pre-stack data, the resulting increased resolution could be potentially used to map the top and base of the target sandstones or at least to make an interpretation of the target layers with increased geological detail.

Sparse-layer inversion (Zhang and Castagna; 2011) was applied to conditioned pre-stack angle gathers from the La Creciente block on the Lower Magdalena Valley at Northern Colombia, using high-resolution spectral decomposition as an initial model assuming a blocky earth and existing well logs for correlation QC before and after the seismic inversion. In the process, parameters for horizontal continuity and vertical resolution were tested and defined. Control of the input parameters to the inversion is important to avoid blowing up noise or generating false positives on the result: if the horizontal continuity is forced upon the data, existing faults would be eliminated; and if vertical resolution is forced to increase, high-resolution artifacts would appear. QC was performed making use of well-ties, wavelet extraction, wedge modeling comparison, bandpass filtering and wavelet convolution.

3.2 Results and Discussion

In order to evaluate if this method is able to identify seismic events below the $\lambda/4$ original data resolution limit of 120 ft, the tuning thickness of a wedge model for the layers of interest was evaluated and examined. Figure 3.1 shows that the tunning thickness expected in the sparse-layer inversion result is approximately 35 ft, this would be the new practical $\lambda/4$ resolution limit, which is comparable to the expected 30 ft thin sandstone layers packet thickness in Lower Porquero formation.

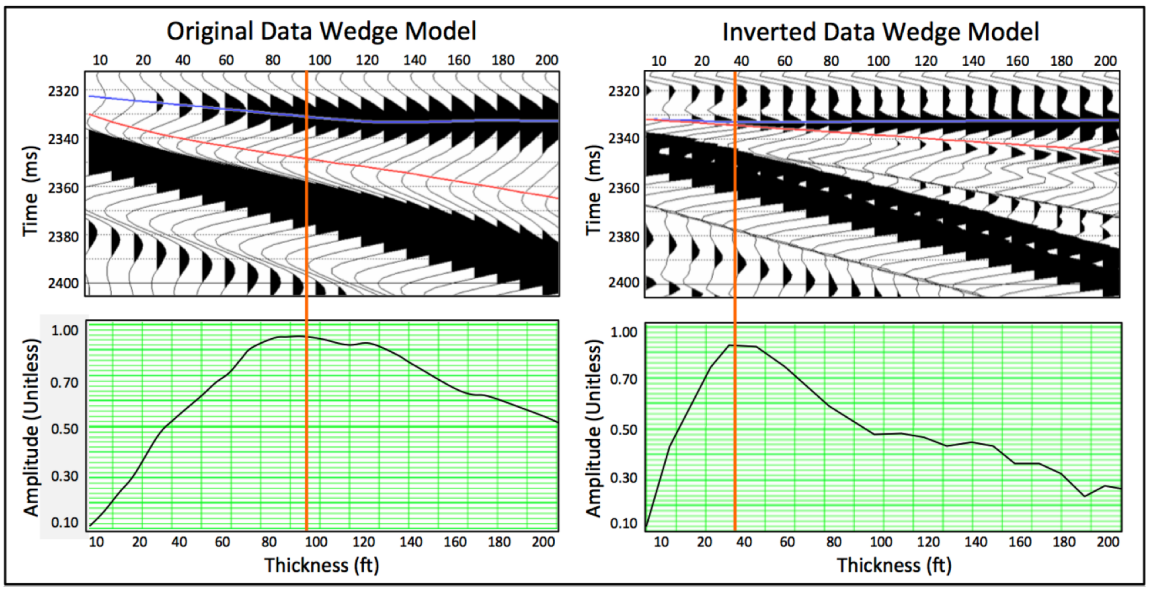

Figure 3.1: Wedge Model Comparison. (Left) Modeled Using extracted wavelet from original data. (Right) Modeled using extracted wavelet from inverted data. Tuning thickness for the original data is approximately 95 ft, tuning thickness for the inverted data is approximately 35 ft. All amplitudes are relative and thus unitless.

The resulting sparse-layer inverted data is consistent geologically and geophysically with the original input data. Geologically, in the sense that by looking at the

layer continuity and location on the inverted data these match the ones on the original data, in Figure 3.2 an arbitrary line was chosen to pass through the available wells.

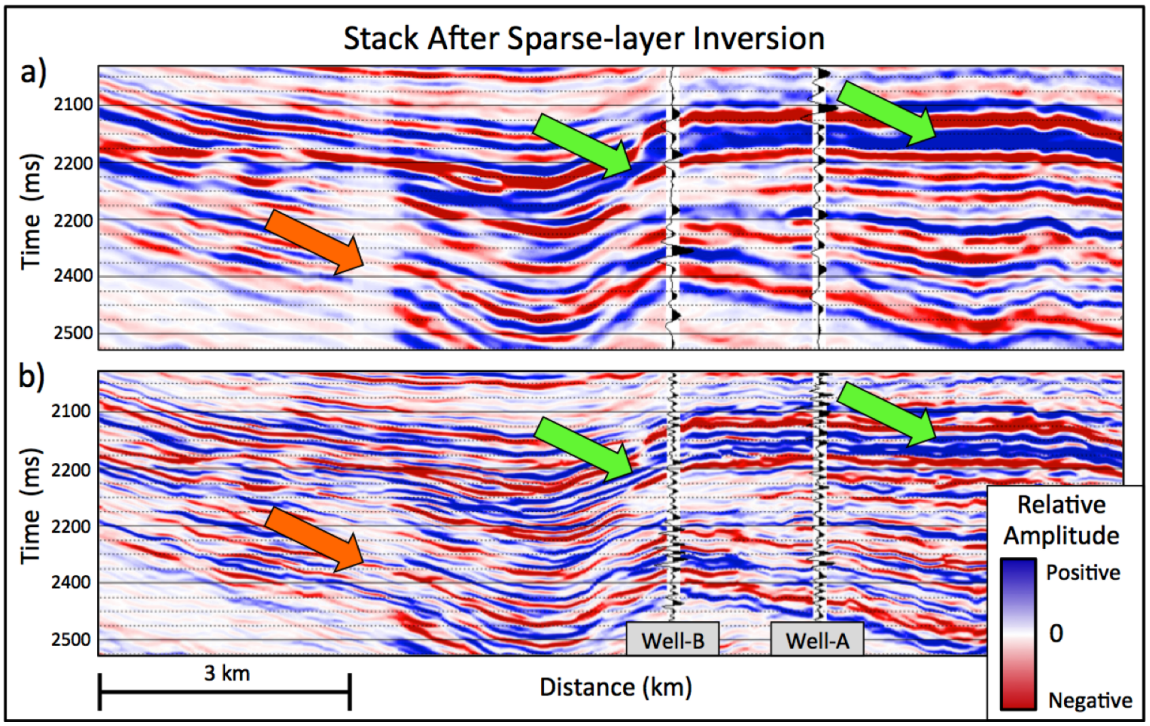

Figure 3.2: (a) Original data stack. (b) Sparse-layer inverted data stack. New interbedded features are observed (green arrows), in the low fold areas previously not seen continuous layers appear (orange arrows). All amplitudes are relative and thus unitless.

The spare layer inversion is geophysically consistent when compared to modeled synthetic traces at existing wells. In particular, for the area of interest at Well-B and Well-C, the inverted seismic results show events that did not appear in the original input data and are now visible, and most importantly coincide with the modeled synthetic trace, Figure 3.3 shows the area of interest at Well-B.

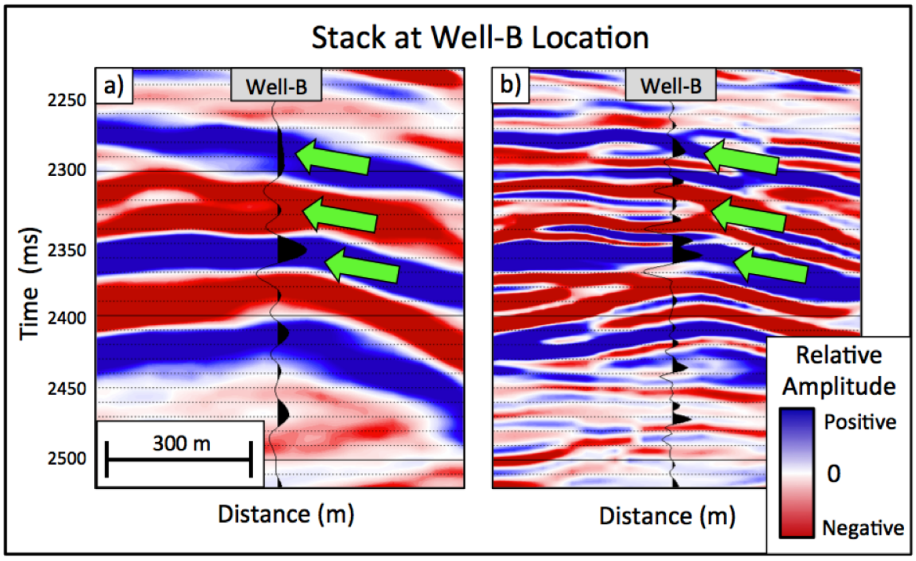

Figure 3.3: Sparse-layer Inverted Data at Well-B. (a) Original Data at Well-B location. (b) Sparse-layer inverted data at Well-B location. Notice that what seems to be continuous layers on the original data are now appearing as interbedded layers on the inverted results (green arrows indicate some of them). All amplitudes are relative and thus unitless.

A good way of validating the sparse-layer inverted data is to show that in itself it preserves the input seismic volume; two ways of corroborating this are: one, to apply a bandpass filter on the inverted data to shape it to the conditioned seismic data frequency amplitude spectrum; and two, to convolve the sparse-layer volume with a wavelet extracted from the input seismic volume. Figure 3.4 compares the original seismic section around Well-B with both cases. Although the results are not identical (they have no reason to be) the overall structural behavior and layer content is similar and consistent with the input data on after both processes.

AVO gradient analysis was done at the well location at the target depth to compare the AVO behavior between the input seismic data and the result from the

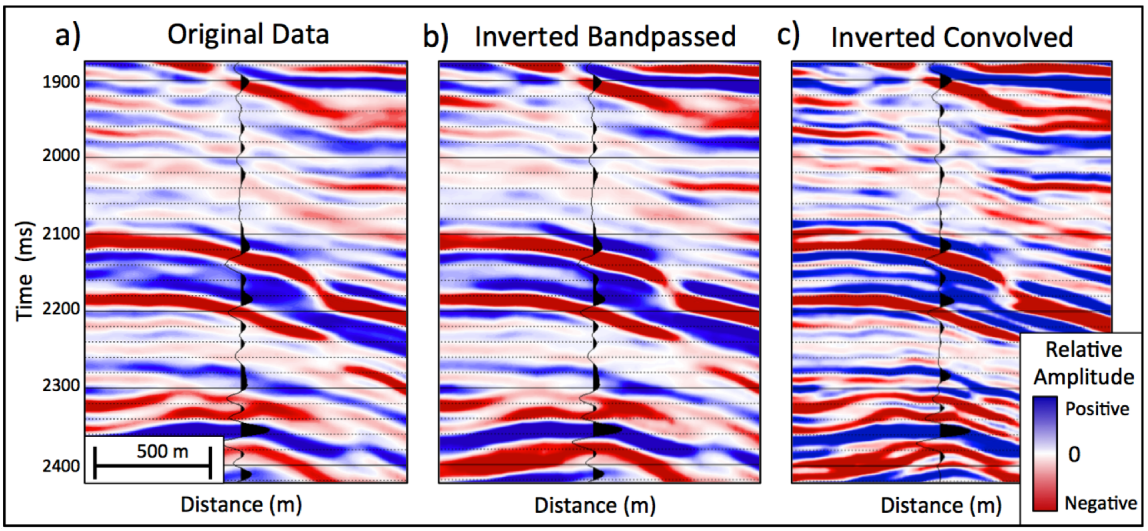

Figure 3.4: Quality Control at Well-B Location. (a) Original seismic data. (b) Inverted data spectrum shaped to match original data. (c) Inverted data convolved with original data wavelet. Inserted synthetic trace corresponds to Well-B location. Notice all three vertical sections have similar consistent geological behavior. All amplitudes are relative and thus unitless.

sparse-layer inversion process. Figure 3.5 shows that the AVO response was preserved during the sparse-layer reflectivity inversion.

The most important result of this thesis work comes from comparing the additional layers in the inverted data with the mud logs at the area of interest. Comparison at Well-B in Figure 3.6 shows an improved resolution in the existing seismic event and two additional events previously not visible that coincide with the thin sandstone layer packet with presence of gas seen in the mud log.

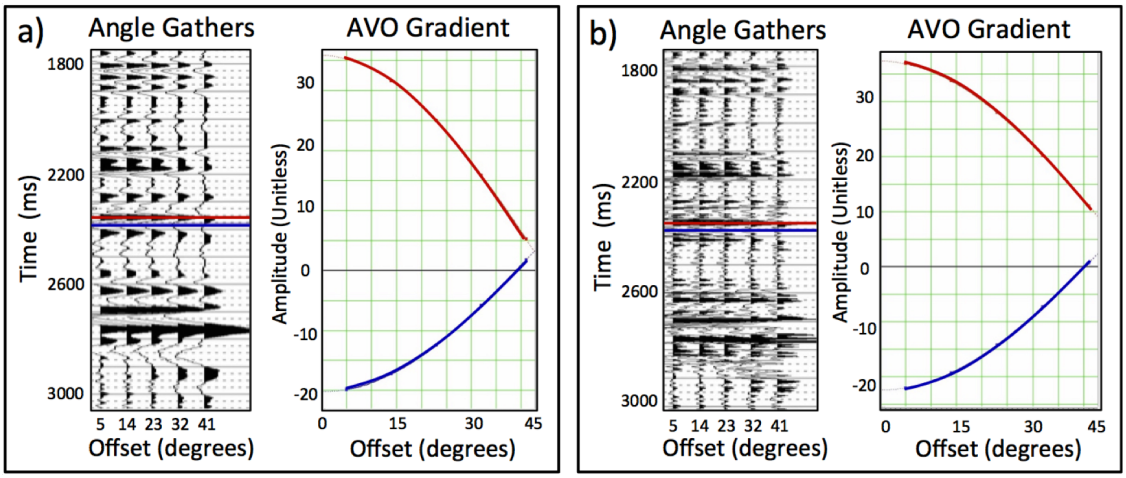

Figure 3.5: AVO Gradient Analysis. a) Original data at Well-B 2350 ms. b) Inverted data at Well-B 2350 ms. Notice AVO behavior is preserved during the sparse-layer inversion. Red curve is the least-mean-squared fit to the amplitude values sampled at the top seismic event (red horizontal line). Blue curve is the least-mean-squared fit to the amplitude values sampled at the bottom seismic event (blue horizontal line). All amplitudes are relative and thus unitless.

Horizon picking was done in the area of interest on the original data and then superimposed on the inverted seismic data (Figure 3.7). It is possible to notice that what seemed to be a continuous seismic event in the original data now exhibits many previously unseen stratigraphic features, some of which pinch-out up-dip and might present good opportunities for further hydrocarbon exploration in the future.

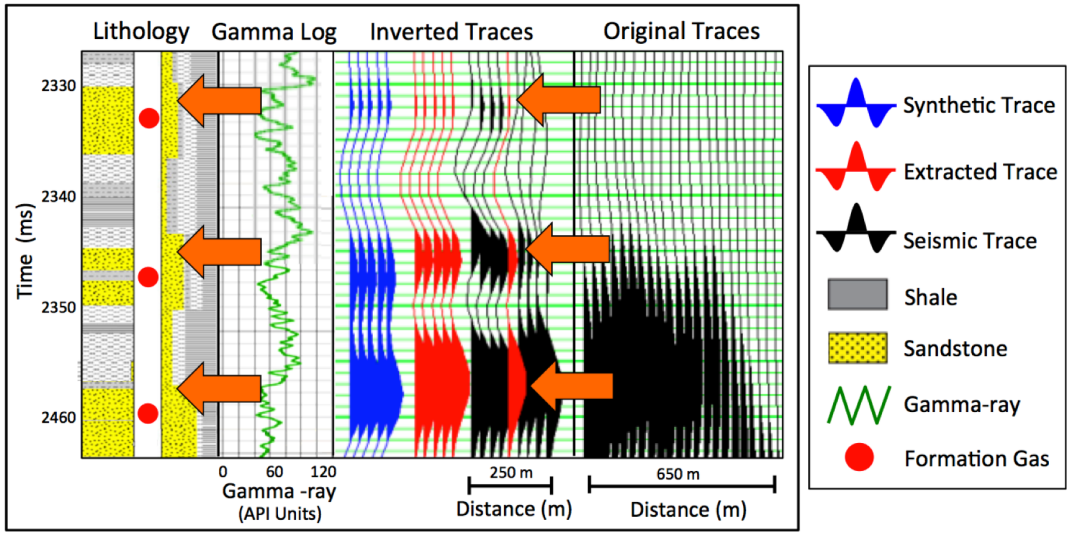

Figure 3.6: Sparse-layer Inverted Data Correlation with Mud log. Orange arrows indicate previously unseen layers on the sparse-layer reflectivity inversion data that coincide with the thin sandstone layers detected.

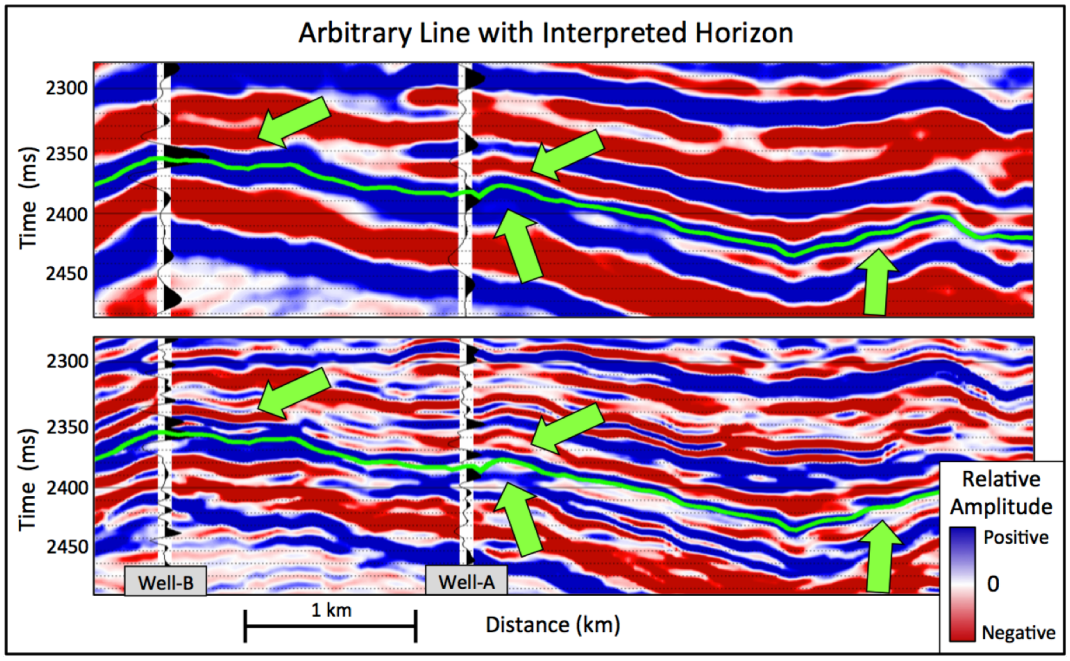

Figure 3.7: Arbitrary line cross-section trough wells of interest. (Top) Original data. (Bottom) Inverted data. Green horizon interpreted on original section superimposed on inverted section, notice on inverted section previously unseen interbedded features (green arrows). All amplitudes are relative and thus unitless.

Chapter 4

Conclusion

4.1 Conclusions

Before attempting a seismic inversion process, a data-conditioning sequence should be tailored to the characteristics and features of the seismic data. During conditioning, it is necessary to oversee all the parameters and QC each one of the steps involved to guarantee the best removal of noise without losing valuable seismic information. The compulsory need of data conditioning previous to sparse-layer reflectivity inversion process comes from the fact that if random noise and multiple reflections go into the seismic inversion algorithm the increased high-frequency content in the output will come mostly from blown-up noise rather than from expected high-resolution seismic events.

Sparse-layer reflectivity inversion is an effective method for improving layer detection on seismic data below conventional resolution, being consistent with original input data and existing well log information and advantageous while it does not depend of a priori models or supporting well log data.

Sparse layer reflectivity inversion method when implemented on data from La Creciente block in the Lower Magdalena valley was able to unveil existing thin sandstone layers previously not seen on the original seismic data that correlate with the gas containing thin sandstone layers in the Lower Porquero formation.

References

Agencia Nacional de Hidrocarburos, 2007, Colombian Sedimentary Basins: Nomenclature, Boundaries and Petroleum Geology, a New Proposal, ANH, 76-78.

Castagna, J. P., M. L. Batzle, and R. L. Eastwood, 1985, Relationships between compressional-wave and shear-wave velocities in clastic silicate rocks: Geophysics, 50, 571-581.

Chopra, S. and J. Castagna, 2014, AVO: Investigation in Geophysics, 16, 86.

Chopra, S. and K. J. Marfurt, 2007, Seismic attributes for prospect identification and reservoir characterization: SEG Books, 50-52.

Estrada, J., P. Aaron, and R. Eden, 2016, Target-oriented data conditioning for prestack inversion in an unconventional reservoir: A Canadian case study: Interpretation, 4, SG11-SG18.

Feng, H and J. C. Bancroft, 2006, AVO principles, processing and inversion: CREWES Research Report, 18, 10.

Gardner, G.H.F, L. W. Gardner, and A. R. Gregory, 1974, Formation velocity and density-the diagnostic basics for stratigraphic traps: Geophysics, 39, 770-780.

Marfurt, K. J., and R. L. Kirlin, 2001, Narrow-band spectral analysis and thin-bed tuning: Geophysics, 66, 1274-1283.

Partyka, G. A., J. A. Gridley, and J. A. Lopez, 1999, Interpretational aspects of spectral decomposition in reservoir characterization: The Leading Edge, 18, 352-360.

Puryear, C. I., and J. P. Castagna, 2008, Layer-thickness determination and stratigraphic interpretation using spectral inversion: Geophysics, 73, R37-R48.

Schmidt, D., A. Veronesi, F. Delbecq, and J. Durant, 2013, Seismic data preconditioning for improved reservoir characterization (Inversion and Fracture Analysis): Presented at GeoConvenion 2013.

Singleton, S., 2009, The effects of seismic data conditioning on prestack simultaneous impedance inversion: The Leading Edge, 28, 260-267.

Zhang, B., D. Chang, T. Lin and K.J. Marfurt, 2015, Improving the quality of prestack inversion by prestack data conditioning: Interpretation, 3, T5-T12.

Zhang, B., T. Lin and K.J. Marfurt, 2015, Noise suppression of time migrates gathers using prestack structure oriented filtering: SEG Technical Expanded Abstracts, 4678-4682.

Zhang, R. and J. P. Castagna, 2011, Seismic sparse-layer reflectivity inversion using basis pursuit decomposition: Geophysics, 76, R147-R158.

Widess, M. B., 1985, How thin is a thin bed?: Geophysics, 50, 2061-2065.